

This work was written as part of one of the author's official duties as an Employee of the United States Government and is therefore a work of the United States Government. In accordance with 17 U.S.C. 105, no copyright protection is available for such works under U.S. Law. Access to this work was provided by the University of Maryland, Baltimore County (UMBC) ScholarWorks@UMBC digital repository on the Maryland Shared Open Access (MD-SOAR) platform.

Please provide feedback

Please support the ScholarWorks@UMBC repository by emailing scholarworks-group@umbc.edu and telling us what having access to this work means to you and why it's important to you. Thank you.

Phase-matched second harmonic generation at the Dirac point of a 2-D photonic crystal.

Nadia Mattiucci,¹ Mark J. Bloemer,² and Giuseppe D'Aguanno^{1,3,*}

¹Aegis Tech., Nanogenesis Division 410 Jan Davis Dr, Huntsville, AL 35806, USA

²Dept. of the Army, Charles M. Bowden Facility, Redstone Arsenal, AL 35898, USA

³gdaguanno@nanogenesisgroup.com

giuseppe.daguanno@us.army.mil

Abstract: We study second harmonic generation in a 2-D photonic crystal with the pump field tuned at the Dirac point of the structure. The simultaneous generation of both forward and backward phase-matched second harmonic is achieved by exploiting a peculiar regime in which the interacting waves have zero phase velocity in the lattice. This regime can be attained even when strong material dispersion is present and therefore lends itself well to be implemented in semiconductor-based frequency conversion devices. A comparison between this method and the quasi-phase-matching technique is also presented.

2014 Optical Society of America

OCIS codes: (160.5298) Photonic crystals; (230.4320) Nonlinear optical devices; (160.0160) Materials; Graphene-like photonic materials.

References and links

1. P. A. Franken, A. E. Hill, C. W. Peters, and G. Weinreich, "Generation of Optical Harmonics," *Phys. Rev. Lett.* **7**(4), 118–119 (1961).
2. J. A. Giordmaine, "Mixing of Light Beams in Crystals," *Phys. Rev. Lett.* **8**(1), 19–20 (1962).
3. P. D. Maker, R. W. Terhune, M. Nisenoff, and C. M. Savage, "Effects of Dispersion and Focusing on the Production of Optical Harmonics," *Phys. Rev. Lett.* **8**(1), 21–22 (1962).
4. M. M. Fejer, G. A. Magel, D. H. Jundt, and R. L. Byer, "Quasi-Phase-Matched Second Harmonic Generation: Tuning and Tolerances," *IEEE J. Quantum Electron.* **28**(11), 2631–2654 (1992).
5. G. D'Aguanno, N. Mattiucci, M. J. Bloemer, and M. Scalora, "Large Enhancement of Interface Second-Harmonic Generation Near the Zero-n Gap of a Negative-Index Bragg Grating," *Phys. Rev. E Stat. Nonlin. Soft Matter Phys.* **73**(3), 036603 (2006).
6. G. D'Aguanno, N. Mattiucci, M. Scalora, and M. J. Bloemer, "Second-Harmonic Generation at Angular Incidence in a Negative-Positive Index Photonic Band-Gap Structure," *Phys. Rev. E Stat. Nonlin. Soft Matter Phys.* **74**(2), 026608 (2006).
7. M. A. Vincenti, D. de Ceglia, J. W. Haus, and M. Scalora, "Harmonic generation in multiresonant plasma films," *Phys. Rev. A* **88**(4), 043812 (2013).
8. D. de Ceglia, S. Campione, M. A. Vincenti, F. Capolino, and M. Scalora, "Low-damping epsilon-near-zero slabs: Nonlinear and nonlocal optical properties," *Phys. Rev. B* **87**(15), 155140 (2013).
9. H. Suchowski, K. O'Brien, Z. J. Wong, A. Salandrino, X. Yin, and X. Zhang, "Phase Mismatch-Free Nonlinear Propagation in Optical Zero-Index Materials," *Science* **342**(6163), 1223–1226 (2013).
10. E. Yablonovitch, "Inhibited spontaneous emission in solid-state physics and electronics," *Phys. Rev. Lett.* **58**(20), 2059–2062 (1987).
11. S. John, "Strong localization of photons in certain disordered dielectric superlattices," *Phys. Rev. Lett.* **58**(23), 2486–2489 (1987).
12. J. D. Joannopoulos, R. D. Meade, and J. N. Winn, *Photonic Crystals, Molding the Flow of Light*. (Princeton University, 1995).
13. J. M. Lourtioz, H. Benisty, V. Berger, J.-M. Gérard, D. Maystre, and A. Tchebnokov, *Photonic Crystals*, (Springer, 2005).
14. Y. S. Kivshar and G. P. Agrawal, *Optical Solitons: From Fibers to Photonic Crystals* (Academic, 2003).
15. N. Bloembergen and A. J. Sieveres, "Nonlinear Optical Properties of Periodic Laminar Structures," *Appl. Phys. Lett.* **17**(11), 483–486 (1970).
16. C. L. Tang and P. P. Bey, "Phase Matching in Second-Harmonic Generation Using Artificial Periodic Structures," *IEEE J. Quantum Electron.* **9**(1), 9–17 (1973).
17. J. P. van der Ziel and M. Ilegems, "Optical second harmonic generation in periodic multilayer GaAs-Al_{0.3}Ga_{0.7}As structures," *Appl. Phys. Lett.* **28**(8), 437–439 (1976).

18. C. M. Bowden and A. M. Zheltikov, "Nonlinear Optics of Photonic Crystals," *J. Opt. Soc. Am. B* **19**(9), 2046–2048 (2002).
19. E. Centeno, "Second-harmonic superprism effect in photonic crystals," *Opt. Lett.* **30**(9), 1054–1056 (2005).
20. K. S. Novoselov, A. K. Geim, S. V. Morozov, D. Jiang, M. I. Katsnelson, I. V. Grigorieva, S. V. Dubonos, and A. A. Firsov, "Two-dimensional gas of massless Dirac fermions in graphene," *Nature* **438**(7065), 197–200 (2005).
21. A. H. Neto, F. Guinea, N. M. R. Peres, K. S. Novoselov, and A. K. Geim, "The electronic properties of graphene," *Rev. Mod. Phys.* **81**(1), 109–162 (2009).
22. F. D. M. Haldane and S. Raghu, "Possible Realization of Directional Optical Waveguides in Photonic Crystals with Broken Time-Reversal Symmetry," *Phys. Rev. Lett.* **100**(1), 013904 (2008).
23. S. Raghu and F. D. M. Haldane, "Analogues of quantum-Hall-effect edge states in photonic crystals," *Phys. Rev. A* **78**(3), 033834 (2008).
24. R. A. Sepkhanov, Ya. B. Bazaliy, and C. W. J. Beenakker, "Extremal transmission at the Dirac point of a photonic band structure," *Phys. Rev. A* **75**(6), 063813 (2007).
25. X. Zhang, "Observing *Zitterbewegung* for Photons near the Dirac Point of a Two-Dimensional Photonic Crystal," *Phys. Rev. Lett.* **100**(11), 113903 (2008).
26. M. Diem, T. Koschny, and C. M. Soukoulis, "Transmission in the vicinity of the Dirac point in hexagonal photonic crystals," *Physica B* **405**(14), 2990–2995 (2010).
27. X. Huang, Y. Lai, Z. H. Hang, H. Zheng, and C. T. Chan, "Dirac cones induced by accidental degeneracy in photonic crystals and zero-refractive-index materials," *Nat. Mater.* **10**(8), 582–586 (2011).
28. K. Sakoda, "Double Dirac cones in triangular-lattice metamaterials," *Opt. Express* **20**(9), 9925–9939 (2012).
29. G. D'Aguanno, N. Mattiucci, C. Conti, and M. J. Bloemer, "Field localization and enhancement near the Dirac point of a finite defectless photonic crystal," *Phys. Rev. B* **87**(8), 085135 (2013).
30. N. Mattiucci, M. J. Bloemer, and G. D'Aguanno, "All-optical bistability and switching near the Dirac point of a 2-D photonic crystal," *Opt. Express* **21**(10), 11862–11868 (2013).
31. *Handbook of Optical Constants of Solids*, E. D. Palik ed. (Academic Inc., 1991).
32. L. Li, "Formulation and comparison of two recursive matrix algorithms for modeling layered diffraction gratings," *J. Opt. Soc. Am. A* **13**(5), 1024–1035 (1996).
33. B. Gralak, S. Enoch, and G. Tayeb, "Anomalous refractive properties of photonic crystals," *J. Opt. Soc. Am. A* **17**(6), 1012–1020 (2000).
34. G. D'Aguanno, M. Centini, M. Scalora, C. Sibilia, M. Bertolotti, M. J. Bloemer, and C. M. Bowden, "Generalized coupled-mode theory for $\chi^{(2)}$ interactions in finite multilayered structures," *J. Opt. Soc. Am. B* **19**(9), 2111–2121 (2002).
35. N. Mattiucci, G. D'Aguanno, M. Scalora, and M. J. Bloemer, "Coherence Length during a SH Generation Process in Nonlinear, One-Dimensional, Finite, Multilayered Structures," *J. Opt. Soc. Am. B* **24**, 877–886 (2007).

1. Introduction

Increasing the coherence length of frequency conversion processes has always been one of the main objectives in the field of nonlinear optics since the experiment of *Franken* and associates [1] in which an extremely small fraction of photons of a ruby laser beam (694 nm) was converted into ultraviolet light (347 nm) at twice the frequency, after the beam was propagated through a quartz crystal. It was soon realized that the poor conversion efficiency had to be ascribed to the normal material dispersion which caused the fundamental and second harmonic waves to travel along the crystal with different phase velocities. Under these circumstances, the second harmonic (SH) field radiated by the oscillating dipoles induced by the fundamental frequency (FF) field can add together constructively only over the coherence length $l_c = \pi/|\Delta k|$, where $\Delta k = (2\omega/c)(n_{2\omega} - n_{\omega})$ is the momentum mismatch (or phase mismatch), n_{ω} and $n_{2\omega}$ are respectively the refractive index of the material at the FF and SH. Shortly after *Franken* and associates experiment [1], *Giordamaine* [2] and *Maker et al.* [3] simultaneously proposed a way to match the phase velocities of the waves at the FF and SH based on the anisotropy properties of certain birefringent crystals, such as potassium dihydrogen phosphate (KDP). The use of birefringent crystals is the most common method to achieve phase matching. More recently, another technique, quasi-phase-matching (QPM), has become extensively utilized [4]. In the QPM approach the correction to the relative phase mismatch between the FF and SH is achieved by periodically alternating the domains of the quadratic nonlinearity. Harmonic generation has also been examined in epsilon-near-zero materials during the past [5,6] and recent [7–9] years. Another approach to achieve phase matching is offered by photonic crystals. Photonic crystals (PCs) or photonic band gap

structures (PBGs) [10–14] can in general be described as structures in which a periodic variation of the linear refractive index of the medium in 1-D, 2-D or 3-D gives rise to allowed and forbidden band for photons in essentially the same way that semiconductors do for electrons. For the FF and SH waves interacting in the periodic lattice, the momentum mismatch can be compensated by the reciprocal lattice vectors of the crystal itself as:

$$\vec{K}_\beta(2\omega) \mp 2\vec{K}_\beta(\omega) = \vec{G}, \quad (1)$$

where \vec{K}_β is the Bloch vector, \vec{G} one of the reciprocal lattice vectors. In Eq. (1) the minus sign refers to the phase matching between the forward propagating pump and the forward propagating SH (forward phase matching), while the plus sign refers to the phase matching between the forward propagating pump and the backward propagating SH (backward phase matching). In 1-D, the possibility to compensate the momentum mismatch using simple periodic multilayered structures (or Bragg reflectors) had been already pointed out in several seminal works [15–17], although, undoubtedly, the subject took a new life soon after the advent of PCs [18,19]. Very recently, the discovery of graphene [20], a purely two-dimensional electronic system where the conduction band and the valence band touch each other at the Dirac point leading to remarkable electronic transport properties [21], has triggered a great deal of new research activity aimed toward the experimental and theoretical study of Dirac points in 2-D PCs [22–28]. In the case of PCs, two photonic bands touch as a pair of cones (Dirac cones) giving rise to a linear, instead of a parabolic, dispersion for photons. Among other things, these structures have been demonstrated to have several analogies with impedance matched metamaterials possessing simultaneously zero effective permittivity and permeability [27,28]. In two recent publications we have studied the anomalous field localization properties in the stop band of a 2-D PC made of an array of dielectric columns near its Dirac point [29] and also the all-optical switching properties [30]. In this work we study phase matched SH generation with the FF field tuned at the Dirac point of a 2-D photonic crystal in the regime in which both the FF and the SH have an effective Bloch vector equal to zero modulus one the reciprocal lattice vectors. This condition provides perfect phase matching for both the forward and the backward generated SH and can be achieved by adjusting the geometrical details of the PC. In Section 2 we utilize the band structure of an infinite lattice as a guide for designing a realistic finite-size lattice and detail the main results of our study followed by a discussion and in Section 3 we present our conclusions.

2. Results and discussion

In Fig. 1 we show the PC structure studied.

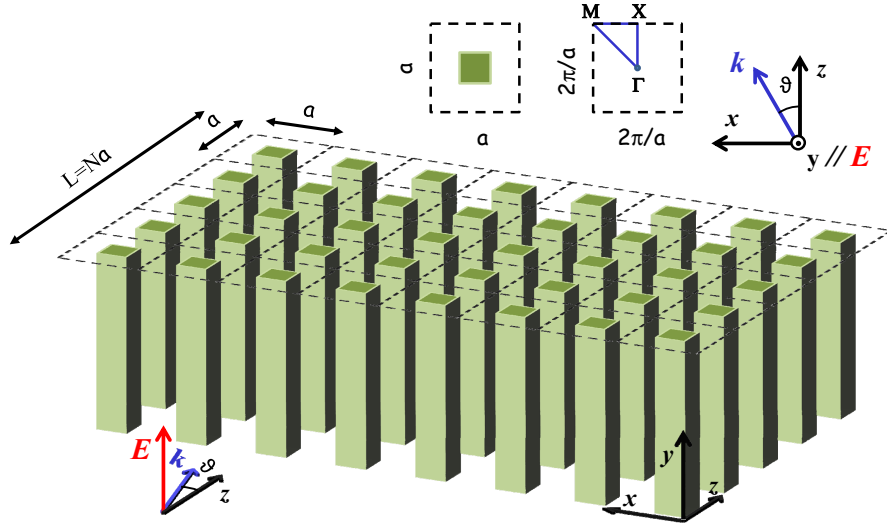


Fig. 1. 2-D PC consisting of a square array (period a) of square dielectric columns of side d . The structure possesses a finite number of rows N along the z -direction and a total length $L = Na$. We suppose that the columns are made of a quadratic material with a generic quadratic coefficient $d^{(2)}$. The pump field is a plane electromagnetic wave with the electric field parallel to the axis of the columns and is incident on the structure with its k -vector in the (x,z) plane (in-plane coupling) forming an angle ϑ with respect to the z -direction.

In Fig. 2 we show the photonic band gap structure of the infinitely periodic lattice with $d/a = 0.35$. The structure admits a Dirac point at $\omega a/2\pi c \approx 0.53$ on the Γ point (i.e. for normal incidence). Two branches of linear dispersion intersect at the Γ point, an additional flat branch is also present corresponding to quasi-longitudinal modes. This sort of topological dispersion around the Dirac point is quite common not only for 2-D square lattices [27], but also for different lattice arrangements, such as the triangular lattice [28]. For computational speed we have used square columns but similar results can be obtained for circular columns as well.

The simplest way to achieve phase matching in such kinds of structures is to tune the FF on the Γ point corresponding to the Dirac point and allow the SH to be generated on another Γ point (as shown in Fig. 2). This way, the Bloch vector of both FF and SH is zero modulus one of the reciprocal lattice vectors and simultaneous forward and backward phase matching can be achieved according to Eq. (1). In this particular case, we have considered the columns to be made of a linearly dispersive material with refractive index at the FF and SH respectively $n_{\omega} \approx 3.62$ and $n_{2\omega} \approx 3.82$. Those values are in the range of the dispersion in the visible and near-IR of several semiconductor materials [31], for example GaAs has a refractive index of ~ 3.4 at $1.8\mu\text{m}$ and ~ 3.6 at $0.9\mu\text{m}$. While here we do not refer to a specific material in particular, nonetheless we mention that the alignment of the SH at the Γ point may be sought by properly tailoring the geometrical characteristics of the PC, i.e. d/a (or r/a in the case of circular columns) and/or the lattice arrangement, so to compensate the dispersion of the specific material under consideration on a case by case basis.

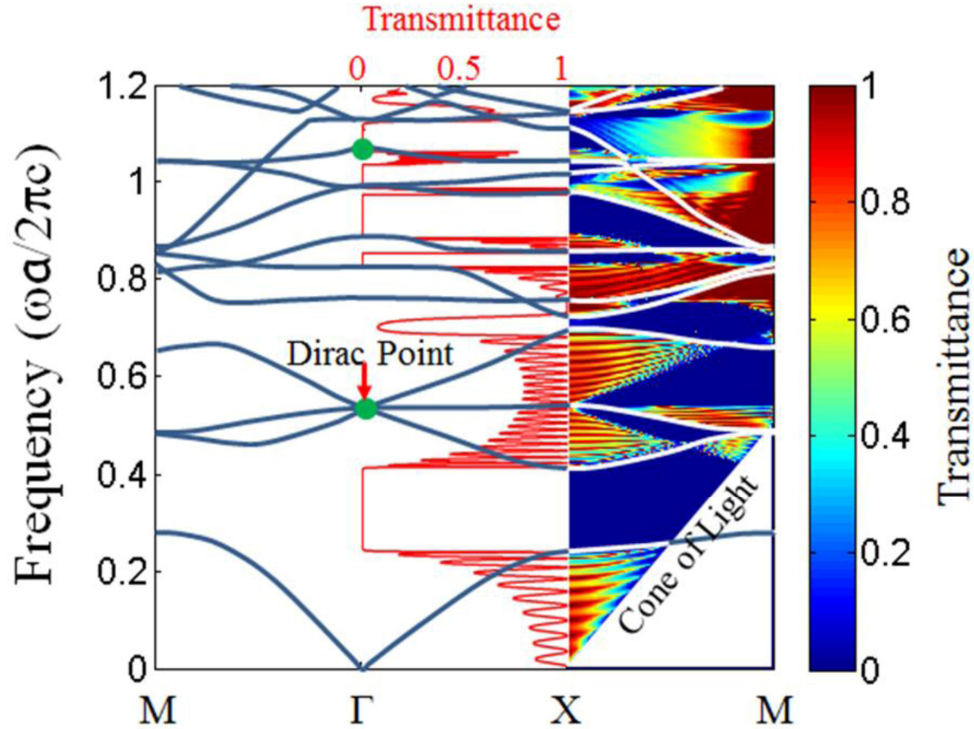


Fig. 2. Photonic band structure of the infinitely periodic square lattice of columns. The normal incidence transmittance (in red) of a finite $N = 10$ period structure is superimposed along the ΓX direction ($k_x = 0$, $0 \leq k_z \leq \pi/a$). The angular transmittance of the same structure is superimposed along the XM direction ($0 \leq k_x \leq \pi/a$, $k_z = \pi/a$). The two green dots indicate respectively the tuning of the FF pump field at the Dirac point and the tuning of the generated SH field. Both the FF and SH are tuned on the Γ point. This condition ensures the Bloch vector of both waves to be zero modulus one of the reciprocal lattice vectors.

In Fig. 2 we have superimposed the transmittance, i.e. transmitted power divided incident power, of a finite $N = 10$ period structure onto the photonic band structure of the infinitely periodic lattice. It is noted that the Dirac point is exactly located at the center of the second pass band of the finite structure at normal incidence. The numerical calculation of the transmittance has been performed using an in-house developed code based on the Fourier-modal-method (FMM) [32]. The calculation of the Bloch dispersion has been performed by using another in-house developed code that finds the unitary amplitude complex eigenvalues of the transfer matrix according to the recipe laid out in [33]. In Fig. 3 we highlight the tuning conditions of the FF and SH on the dispersion of the infinitely periodic lattice (3(a) and 3(c)) and on the transmittance of the finite 10-period structure (3(b) and 3(d)).

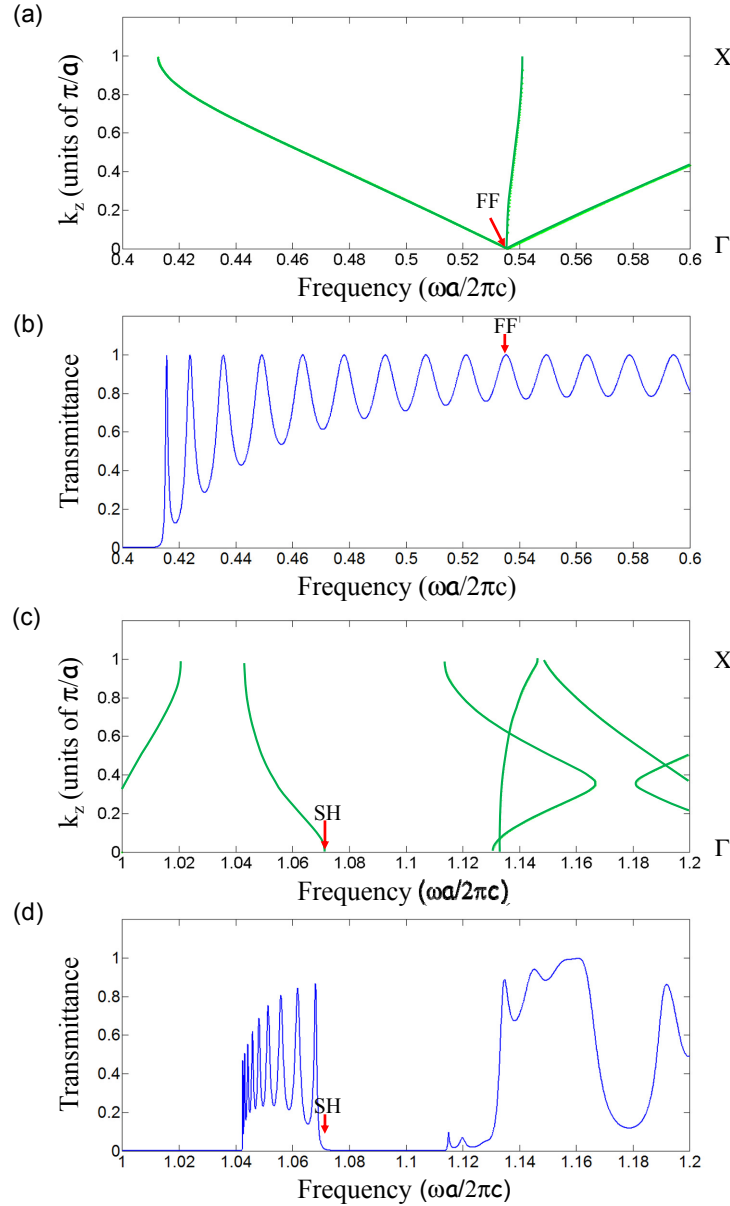


Fig. 3. Tuning conditions for the FF and SH indicated on the dispersion of the infinitely periodic lattice (a) and (c), and on the transmittance of the finite 10-period structure (b) and (d).

The perfect phase matching condition is achieved when the second harmonic is tuned at the band edge. The band edge is always in the region where the transmittance decreases as it approaches the band gap and it should not be confused with the spectral position of the band edge transmission resonance. In this paper we are not exploiting a double resonant condition, i.e the case in which the FF and SH are both tuned on transmission resonances of the structure. In other words, we do not rely on the enhancement of the density of modes at the FF and SH, but we are instead exploring a true phase matching condition where, as we will see in a moment, the conversion efficiency increases as the square of the length of the structure.

In order to confirm the results of the previous analysis, we have calculated the SH conversion efficiency for three topical cases, as exemplified in Fig. 4.

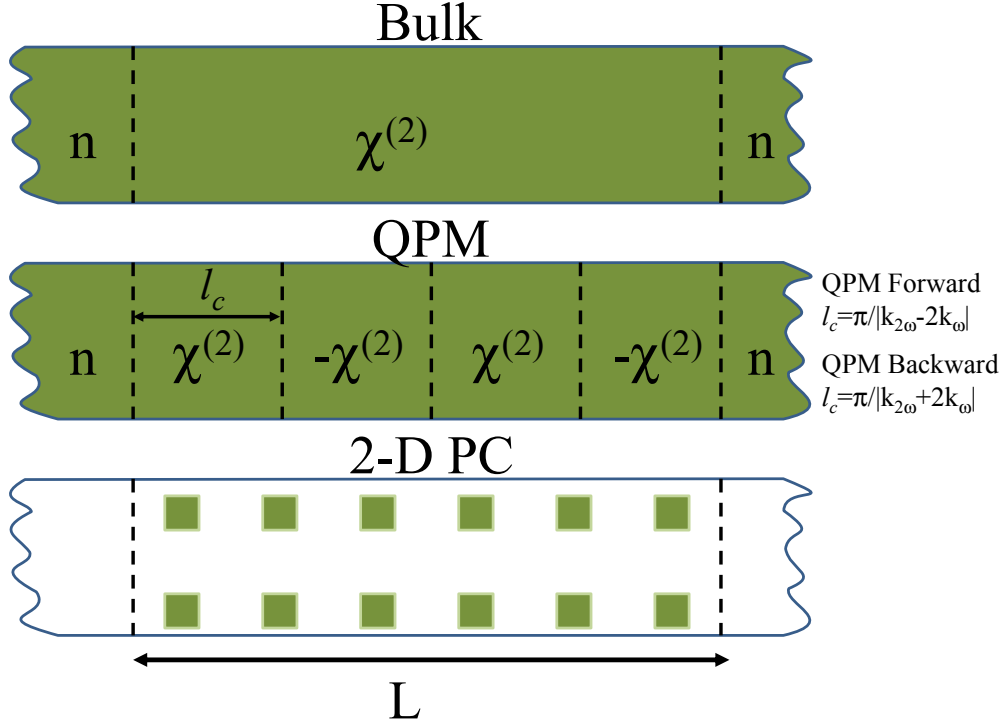


Fig. 4. Schematic sketch of the three cases considered for the calculation of the SH conversion efficiency.

First we consider the conversion efficiency (generated SH power divided incident FF power) of a non-phase-matched bulk medium having a quadratic nonlinearity over a length L , then we consider the conversion efficiency from the same bulk of length L where the QPM technique has been used to compensate the phase mismatch, and, finally, we study the conversion efficiency of the 2-D PC made of the same material and same total length L under the tuning conditions previously elucidated. In the comparison we use the first order QPM, i.e. we periodically invert the sign of the quadratic domains each coherence length [4]. In particular, we have considered two sub-cases: the QPM for the compensation of the phase mismatch of the forward generated SH and the one for the compensation of the phase mismatch of the backward generated SH. Note that the compensation of the phase mismatch of the backward SH is more difficult to achieve experimentally [4] because backward SH coherence length is much smaller than forward SH coherence length and requires an inversion of the sign of the domains on short distances. On the contrary, in the case of the PC, the particular tuning conditions previously reported, i.e. the FF and SH aligned at the Γ point, make possible the simultaneous phase matching of both the forward the backward SH. The conversion efficiency has been calculated by a straightforward extension to 2-D structures of the coupled mode theory for quadratic interactions previously developed for 1-D structures [34]. The results of the calculation are reported in Fig. 5 and Fig. 6 for a value of the quadratic nonlinearity $d^{(2)} = 9\text{pm/V}$, an input intensity of 100MW/cm^2 , and forward coherence length of the bulk material of $\sim 2a$.

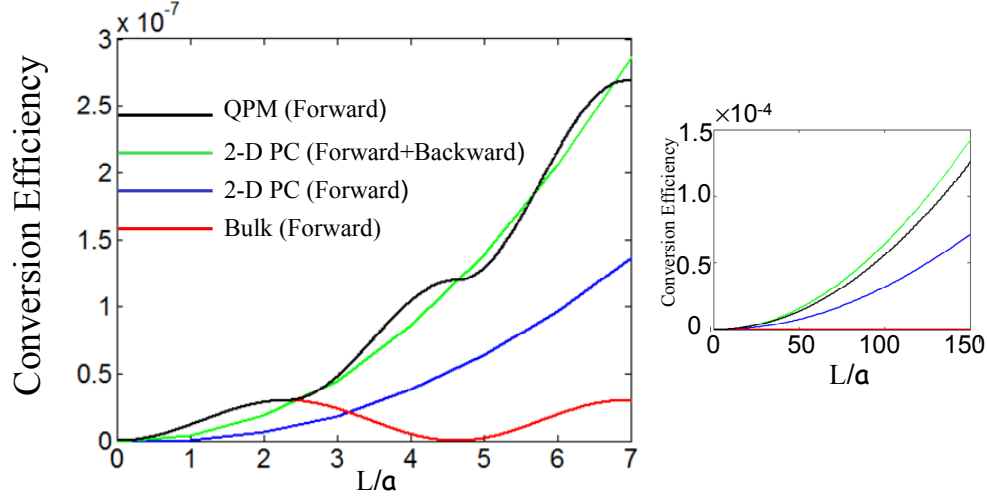


Fig. 5. Conversion efficiency vs. L/a . The main figure shows the oscillations over few elementary cells. The ancillary figure reports the conversion efficiency up to 150 elementary cells. The conversion efficiency scales as L^2 for both the QPM and the PC. In this case the comparison is drawn with the QPM for the forward generated SH.

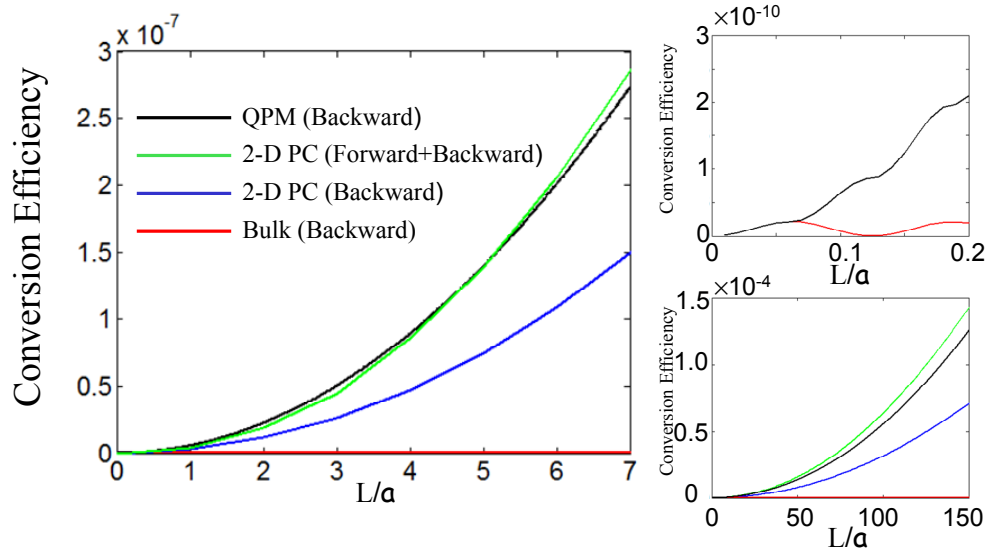


Fig. 6. Conversion efficiency vs. L/a . In this case the comparison is with the QPM for the backward generated SH.

Figures 5 and 6 show how the conversion efficiency for the PC scales exactly as L^2 . This is a clear indication that the generation is happening under perfect phase matching conditions, in agreement with the previous analysis based on the Bloch dispersion. Moreover the backward and forward generated SH are perfectly balanced [35] and the total conversion efficiency (forward + backward) roughly equals the one that is obtained by the QPM technique. If just the forward conversion efficiency is detected, the QPM gives roughly double the conversion efficiency. The comparison with the backward QPM is more a scholastic than a practical case, given the extremely short coherence length of the backward SH which would require an inversion of the quadratic domains over exceptionally small

distances. In this sense the phase matched backward generated SH from the PC represents a truly remarkable result. It is even more significant if we consider that the filling fraction of the quadratic material in the PC is only 10% compared to the 100% in the QPM case. Finally in Fig. 7 we show a snapshot of the FF pump field tuned at the Dirac point and the SH generated field for the 10-period structure. For an animation of the time evolution of the fields see [Media 1](#).

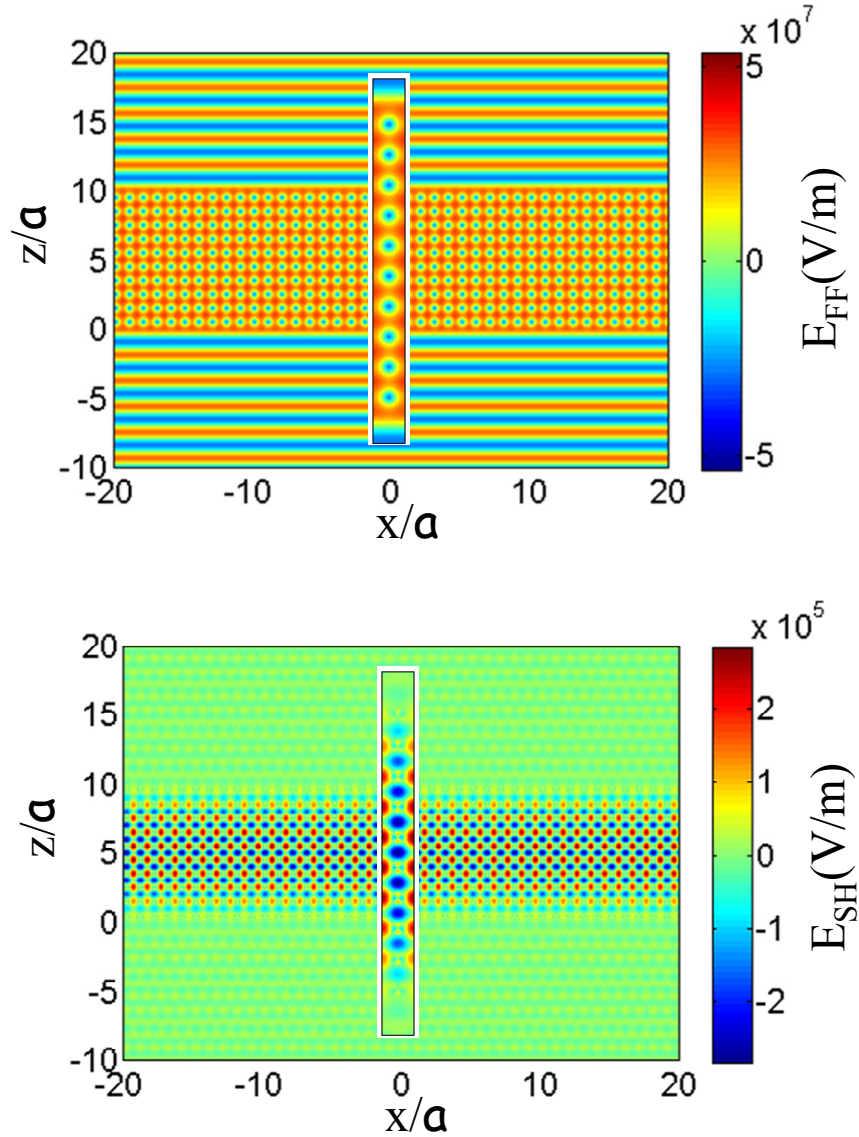


Fig. 7. Snapshot of the FF pump field (upper figure) tuned at the Dirac point and the SH generated field (lower figure) for the 10-period structure. For an animation showing the time evolution see [Media 1](#). The center of both figures reports a magnification of the field localization over one line of columns along the z -axis.

The animation shows how at the Dirac point the photonic crystal basically acts as perfect transparent material, the wave-front of the incident FF field undergoes minimal distortion as it propagates through the crystal and it is completely transmitted, in agreement with previous studies [29]. It is also noted that the SH field is indeed generated perfectly balanced in the forward and backward direction, as one may expect based on the Bloch vector analysis. We have also performed additional calculations for the conversion efficiency when the SH field is slightly misaligned with respect to the Γ point and found that, as expected, the conversion efficiency roughly scales as: $\text{sinc}^2(\Delta K_{\beta}L/2)$ where ΔK_{β} is the Bloch vector mismatch.

3. Conclusions

In conclusion, we have studied phase matched SH generation with the pump field tuned at the Dirac-point of a 2-D photonic crystal. We have shown that perfectly balanced, phase-matched SH emission can be achieved when the SH is aligned at a Γ point of the structure. This procedure can be compatible with the dispersion characteristics of several semiconductor materials by properly tailoring the geometrical characteristics of the PC. Although here we have focused on a square lattice with square columns, similar results can be obtained for different lattice arrangements and/or different shapes of the columns. Moreover, while here we have concentrated our attention on the coupling with both the FF and SH fields polarized parallel to the columns, different coupling conditions can be explored as well, depending on the particular symmetry properties of the quadratic tensor of the material employed. In general, we expect similar results provided that the alignment of the pump and the generated SH respectively at the Dirac point and at the Γ point is attainable. The concepts elucidated in the present work could also be extended to parametric interactions, such as three-wave mixing, with the pump field tuned at the Dirac point and the idler and signal aligned at two Γ points opening new scenarios in the field of nonlinear frequency conversion devices.

Acknowledgments

This work has been supported by DARPA SBIR project number W31P4Q-11-C-0109.